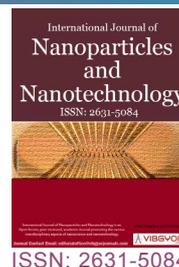# Evaluation of Nano-Antenna Directivity Contributions for EM Propagation in WBANs

Sarah Hussein[1], Abdul Rahman El Falou[1], Walaa Sahyoun[1], Youmni Ziade[1] and Raed M. Shubair[2,3]

[1]*Electrical and Computer Engineering Department, Beirut Arab University, Tripoli, Lebanon*

[2]*Research Laboratory of Electronics, Massachusetts Institute of Technology, Cambridge, MA, USA*

[3]*Electrical and Computer Engineering Department, New York University Abu Dhabi, UAE*

Abstract

In-vivo sensing, diagnosis and treatment of diseases is having a great attention lately. With advanced computational systems, the processing of the biological data as well as the prediction of diagnosis is becoming more promising. However, the implementation of these systems inside the human body has a major challenge: Modeling the communication channel. To overcome this problem, researchers are investigating the main factors that define the characteristics of the communication channel between nano-devices. In this work, a study of the impact of nano-antenna directivity on the electromagnetic propagating wave in the communication channel inside the human body is conducted. Then, these results are compared to the other contributors in the path loss *in-vivo* that are discussed earlier in literature: Frequency and propagation distance. The simulation results show that the nano-antenna directivity seems to have minor contributions (5-7 dB) on the total path loss inside the human body compared to the communication distance (20-30 dB) and the operating frequency (10-15 dB).

Keywords

Path loss, Nano-devices, Nano-antenna directivity, Bio-sensing, THz communication

Introduction

Nowadays, *in-vivo* nano-biosensing is becoming the driver of the biomedical engineering applications. Nano-sensors and nano-devices play a significant role in this evolution. Thanks to these technologies, various tools are developed to control multiple entities at the atomic as well as the molecular levels [1]. Fast and accurate disease diagnosis as well as treatment is now possible thanks to the real time operational capability of nano-sensors inside the human body [2].

Even though the research on nano-devices is having good advancements, the communication between nano-sensors within an *in-vivo* Wireless Body Area Network (iWBAN) still a big problem. On one hand, the researchers are investigating the communication model limitations [3-5]. On the other hand, they are working on the design of

new materials and technologies to be implemented inside the human body [6,7]. Essentially, three models are utilized to undergo the communication process inside the human body: Ultrasound (US) communication [8], molecular communication [9] and electromagnetic communication [10]. The scope of this paper is to evaluate the contribution of nano-antenna directivity in the electromagnetic communication channel operating *in-vivo* at THz frequencies. Then, this contribution is compared to that of the communication distance and the operating frequency. This evaluation is based on the state-of-the art models discussed in literature and mainly, it is an extension of the work presented in [11].

In Section II, we summarize the main elements that contributes in the total path loss encountered in THz band as well as their relation and dependencies to the operating frequency, to the distance traveled by the electromagnetic wave or in other words, the tissue penetration depth and finally, to the nano-antenna directivity. In Section III, we apply the propagation losses models discussed in section II to a simplified human model made of three layers: Water, skin and epidermis. The simulation results for the communication losses in these three layers are shown. In Section IV, an interpretation of the results is performed in order to assess the impact factor of each loss element with respect to the total path loss. Finally, we draw our conclusions and we present our future work and perspectives in Section V.

Propagation Losses

The main factors that affect an electromagnetic wave traveling inside the human body at the THz frequencies are: The spreading of the propagating wave (PL_{Spr}), the molecular absorption from the human tissues (PL_{Abs}), and the scattering of the signal from the biological particles (PL_{Sca}). Therefore, the total path loss (PL_t) is given by

$$PL_t = PL_{Spr} + PL_{Abs} + PL_{Sca} \qquad (1)$$

Spreading loss

As the electromagnetic wave travels through the medium for a certain distance, the spreading of the signal occurs. It still diminishes as it spreads out. Assuming a spherical propagation model and taking into account the nano-antenna gain effect, the spreading of the electromagnetic wave is given by the inverse-squared distance function as

$$PL_{Spr} = -10 \log_{10}\left[D\left(\frac{\lambda_g}{4\pi d}\right)^2 \right] \qquad (2)$$

Where d is the distance traveled by the electromagnetic wave, λ_g is the medium wavelength and D is the nano-antenna directivity. On the other hand, the medium wavelength, λ_g, is the ratio of the free space wavelength λ_0 to the real part of the refractive index of the material n', such that

$$\lambda_g = \lambda_0 / n' \qquad (3)$$

From [12], the antenna directivity D, is the ratio of the maximum power density in W/m^2 to its average value over a sphere. Considering the observation in the far field along with a source with a Gaussian beam, the antenna directivity, D, is hence computed as

$$D = \frac{8}{\left[\frac{8}{3} - \left(\cos\Delta\theta + \cos^2\Delta\theta + \frac{1}{3}\cos^3\Delta\theta \right) \right]} \qquad (4)$$

Where $\Delta\vartheta$ is the Guassian beam width of the nano-antenna.

Absorption loss

In the THz band, the biological molecules are excited by the electromagnetic waves at specific frequencies, this fact causes the vibration of these molecules [13]. Therefore, some of the propagating wave energy is transformed to kinetic energy and hence to heat. Hence, absorption loss can be defined as the fraction of the incident electromagnetic waves which are not able to pass within the human tissue at a given frequency.

For an electromagnetic wave traveling a distance *d* and referring to Beer-Lambert law [14], the loss due to the molecular absorption is given by

$$PL_{Abs} = -10 \log_{10}(e^{-d\mu_{Abs}}) \qquad (5)$$

Where μ_{Abs} is the molecular absorption coefficient which depends on the medium composition and it is given as

$$\mu_{Abs} = \frac{4\pi n''}{\lambda_0} \qquad (6)$$

Where n'' is the imaginary part of the tissue refractive index.

Since we are dealing with a very large number of water molecules for frequencies up to 1 THz, it is recommended to calculate the complex permittivity of the human tissues using the Debye Relaxation

Model [15-17] as

$$\epsilon = \epsilon' - j\epsilon'' \qquad (7)$$

Where ϵ' and ϵ'' are the real and imaginary parts of the complex permittivity given by

$$\epsilon' = \epsilon_\infty + \frac{\epsilon_1 - \epsilon_2}{1 + (\omega\tau_1)^2} + \frac{\epsilon_2 - \epsilon_\infty}{1 + (\omega\tau_2)^2} \qquad (8)$$

And

$$\epsilon'' = \frac{(\epsilon_1 - \epsilon_2)(\omega\tau_1)}{1 + (\omega\tau_1)^2} + \frac{(\epsilon_2 - \epsilon_\infty)(\omega\tau_2)}{1 + (\omega\tau_2)^2} \qquad (9)$$

The values of ϵ_∞, ϵ_1, ϵ_2, t_1 and t_2 for the lower THz band are given in [10] and [12]. Consequently, ϵ' and ϵ'' can be evaluated. On the other hand, the imaginary part of the refractive index, is given by

$$n'' = \sqrt{\frac{\sqrt{\epsilon'^2 + \epsilon''^2} - \epsilon'}{2}} \qquad (10)$$

Thus, μ_{Abs} and PL_{Abs} can be calculated.

Scattering loss

The biological elements of the human body are of different types of composites, such as molecules and cells each having different geometry and different electromagnetic properties. Scattering by particles corresponds to the change of the direction of propagation and phase of the electromagnetic wave after interaction with the microscopic non-uniformities present in the human tissue. Scattering depends on the size, refractive index and shape of the individual particle as well as on the wavelength of the incident beam [18]. In this paper, we consider the scattering from small molecules as well as from large cells compared to the wavelength. Hence, the scattering path loss is

$$PL_{Sca} = -10\log_{10}\left(e^{-\left(\mu_{small} + \mu_{large}\right)d}\right) \qquad (11)$$

Where μ_{small} and μ_{large} are the scattering coefficients for small and large particles respectively and are defined as

$$\mu_{small} = \rho_v Q_{small}\sigma_g \qquad (12)$$

And

$$\mu_{large} = \rho_v Q_{large}\sigma_g \qquad (13)$$

These coefficients depend on the particle concentration ρ_v and the geometric cross section σ_g such that,

$$\rho_v = \frac{k}{\frac{4}{3}\pi r^3} \qquad (14)$$

And

$$\sigma_g = \pi r^2 \qquad (15)$$

Where k is the volume fraction of the particle [19] and r is the radius of the particle.

The absorption coefficient for small particles Q_{small} depends on the scattering efficiency of small particle assuming a spherical absorbing particle modeled by Rayleigh scattering as

$$Q_{small} = \frac{8}{3}\psi^4\,\mathbf{Re}\left(\frac{n^2 - 1}{n^2 + 2}\right)^2 \qquad (16)$$

And

$$\psi = 2\pi r / \lambda_g \qquad (17)$$

Which is the dimensionless size of the particle.

On the other hand, the absorption coefficient for large particles Q_{large} depends on the scattering efficiency of large particles modeled using the anomalous diffraction approximation as

$$Q_{large} = 2 - \frac{4}{p}\sin(p) + \frac{4}{p^2}\left(1 - \cos(p)\right) - \frac{\sigma_{abs}}{\sigma_d} \qquad (18)$$

And

$$p = 4\pi r(n - 1)/\lambda \qquad (19)$$

Which is the phase delay of the wave passing through the center of the particle and σ_{abs} is the molecular absorption cross section.
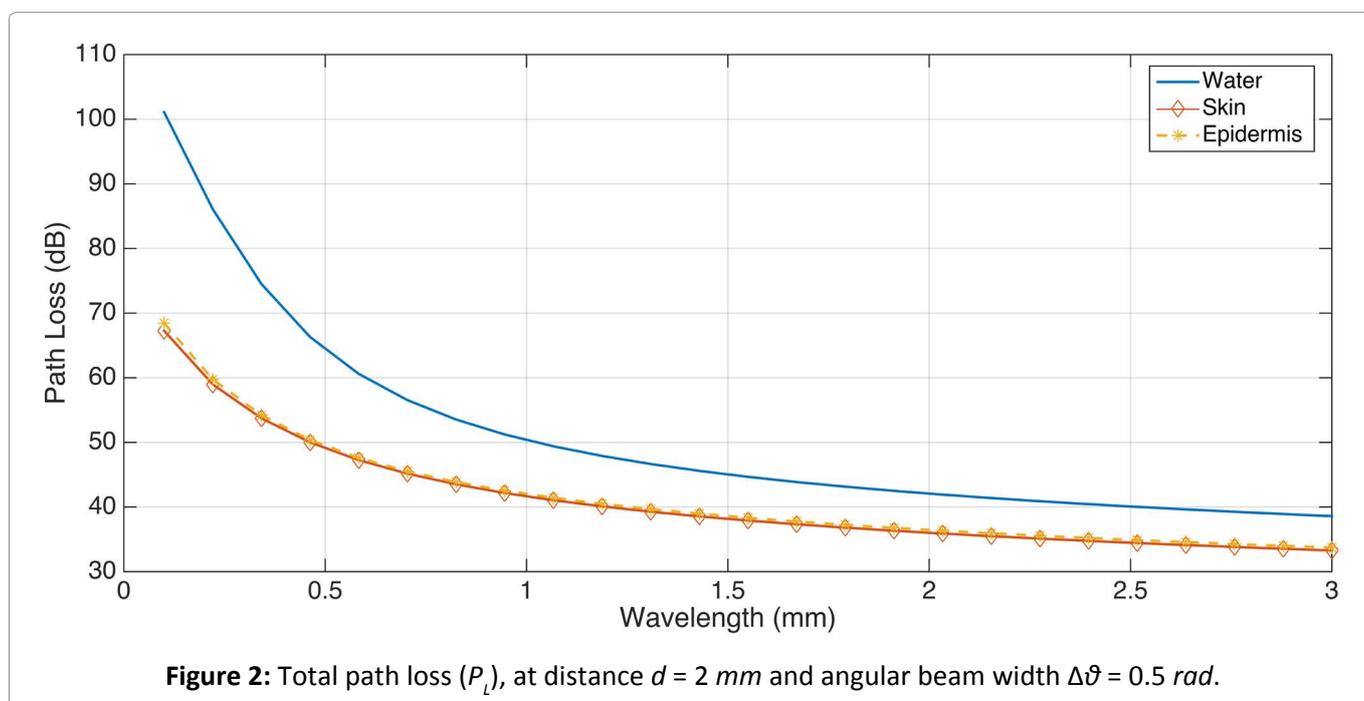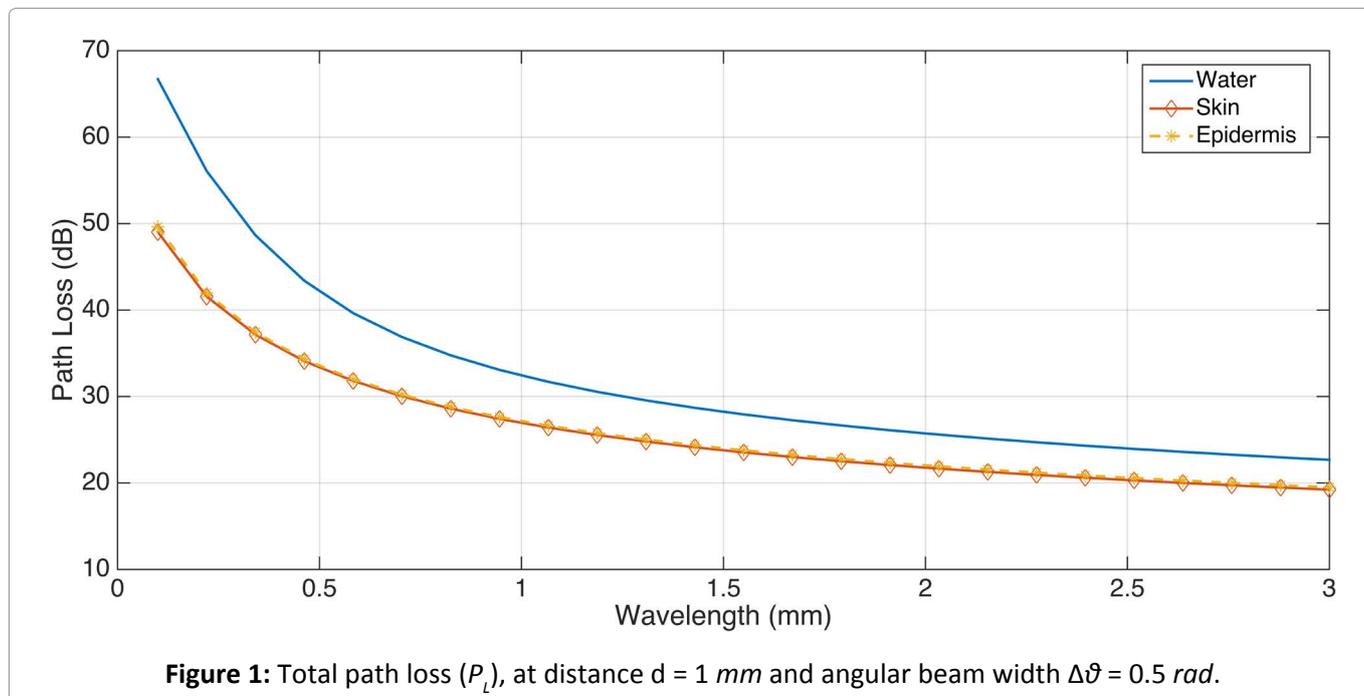
Simulation Results

In this section, we numerically evaluate the analytical models presented in Section II. However, we exclude the scattering loss since it is negligible compared to the absorption and spreading losses. Moreover, we take into account realistic parameters of the intra-body properties [15-17]. In this work, we conduct our analysis for water, skin and epidermis medium which is a simple representation of the human layers that the electromagnetic wave will pass through inside the human body.

Path loss and frequency

Figure 1 and Figure 2 illustrate the total path loss in dB with respect to the medium wavelength for water, skin and epidermis respectively for two different distances, 1 mm and 2 mm.

Similar to conventional communication models

Figure 1: Total path loss (P_L), at distance d = 1 mm and angular beam width $\Delta\vartheta$ = 0.5 rad.

Figure 2: Total path loss (P_L), at distance d = 2 mm and angular beam width $\Delta\vartheta$ = 0.5 rad.

in the megahertz frequency ranges, the total path loss increases with frequency. This finding is expected since it validates the state of- the art models discussed in literature.

Path loss and distance

Figure 3 visualize the total path loss with respect to the communication distance d for water, skin and epidermis respectively. From the figure, we can see that the total path loss increases with distance. It can be noticed also that the path loss due to the propagation in water molecules is much larger than the path loss due to the propagation in skin and epidermis. On the other hand, it is clear that the propagation losses are very similar in the skin and epidermis layers. This finding is expected since both the skin and the epidermis have similar tissue characteristics.

Path loss and nano-antenna directivity

Figure 4 shows the total path loss with respect to the Gaussian Beam Width $\Delta\vartheta$ for water, skin and epidermis respectively.
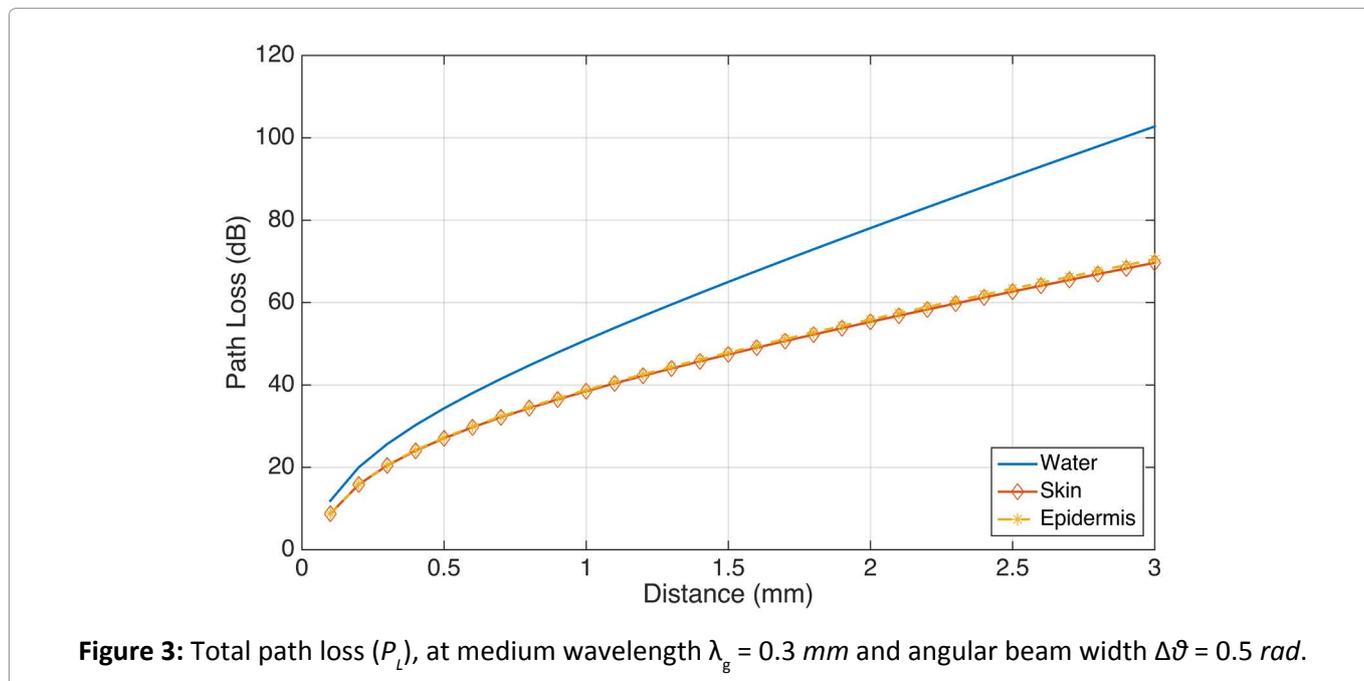
Figure 3: Total path loss (P_L), at medium wavelength λ_g = 0.3 *mm* and angular beam width $\Delta\vartheta$ = 0.5 *rad*.

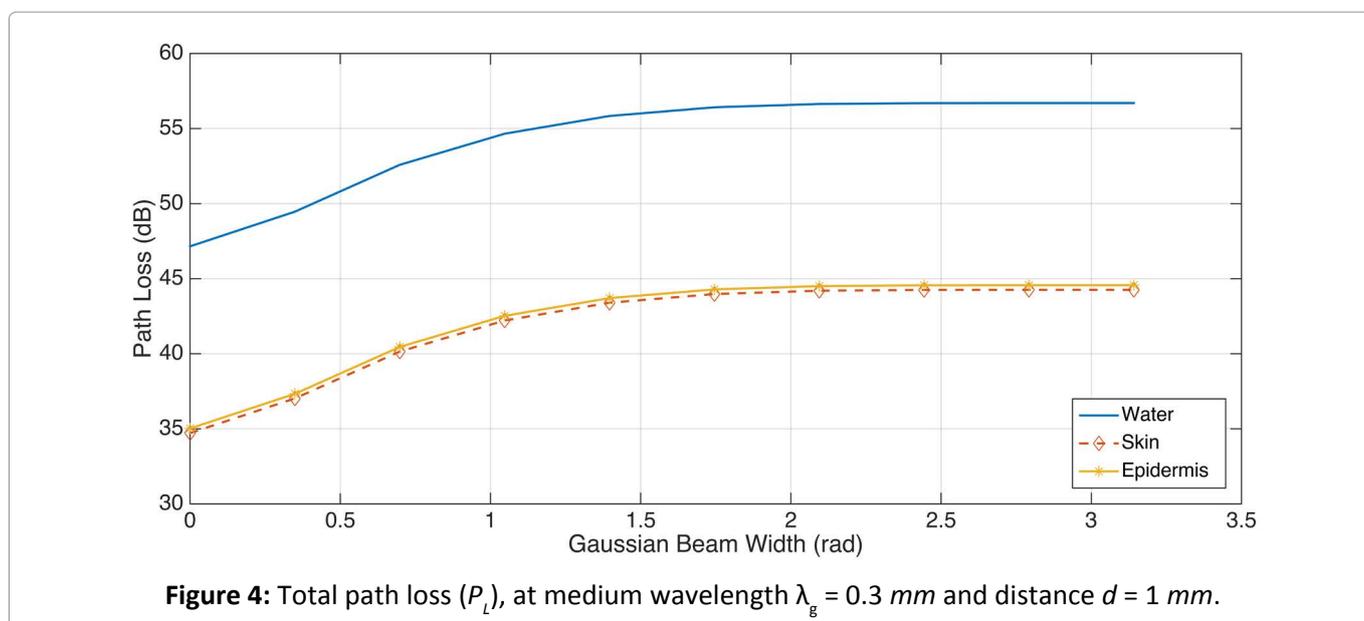**Figure 4:** Total path loss (P_L), at medium wavelength λ_g = 0.3 *mm* and distance d = 1 *mm*.

From the graph, we can see that the path loss increases with large beam width and consequently, decreases with higher directivity.

Discussion

From the numerical results shown in Section III, it is relevant that the path loss increases with frequency and distance. This is expected from the early communication system models discussed in literature.

As for the different propagation losses impact factor, we can see that the absorption loss is governed by the absorption coefficients of the human tissue molecules that is, referring to [15] and [20],

are considerably high at THz frequencies. The reason behind this is the fact that the rotation transition of water molecules is located in this band.

The scattering loss, on the other hand, depends on the radius of the human body particles. The size of the scatterers at THz being much smaller than the wavelength of the propagating THz wave [21,22], negligible scattering loss compared to the absorption loss will result. Therefore, the spreading and absorption losses are the main contributors to the total path loss at THz frequencies.

The relationship between path loss and communication distance is governed by the absorption loss which is, for water molecules, larger

Hussein et al. Int J Nanoparticles Nanotech 2019, 5:032

ISSN: 2631-5084 | • Page 6 of 7 •

than that for skin and epidermis at larger communication distance. Thats why we can see approximately same path loss value at lower distances (< 0.5 mm). However, when the communication distance increases, the curves diverge. The path loss in water (80 dB at 2 mm) is much higher than that of the skin and epidermis (55 dB at 2 mm).

On the other hand, the nano-antenna directivity seems to have a big impact on the communication channel at THz frequencies. From the simulated values, we can see that the increasing the Gaussian beam width from 0 to 1.5 rad increases the path loss by 10 dB approximately for water, skin and epidermis. However, for a beam width between 1.5 and 3 rad, the path loss is approximately constant for each medium. Therefore, we can see that the major impact on path loss is for the communication distance as well as the operating frequency in the human body. These two factors are more critical to consider than the nano-antenna directivity.

It is important also to mention the difference in the path loss between water layer from one side and the skin and epidermis layers from the other side. The water layer exhibited larger path loss than the skin and epidermis. This difference is due to the larger absorption loss encountered in the water layer than in the skin or epidermis.

Conclusion

Nano-networks are exponentially expanding. The electromagnetic communication channel is having more attention and is promising to be adopted in wireless body area networks. However, it needs deep study of its characteristics. In short, the main factors that affect the electromagnetic wave traveling at THz frequencies inside the human body are the nano-antenna directivity, the communication distance and the operating frequency. However, the major impact is that of distance and frequency. Future work involves the design of a more realistic human tissue model to include the blood, the muscles and the bones. Moreover, the study of the path loss at optical frequencies is one of the perspectives due to the different characteristics of the molecules in this band and hence, the effect on the absorption loss.

References

1. I Akyildiz (2010) Nanonetworks: A new frontier in communications. Proceedings of the 2010 International Conference on Security and Cryptography (SE-CRYPT).

2. H Guo, P Johari, J Jornet, Z Sun (2016) Intra-body optical channel modeling for in-vivo wireless nanosensor networks. IEEE Transactions on NanoBioscience 15: 41-52.

3. H Elayan, RM Shubair, J Jornet, P Johari (2017) Terahertz channel model and link budget analysis for intrabody nanoscale communication. IEEE Transactions on NanoBioscience 16: 491-503.

4. RM Shubair, H Elayan (2015) A survey of in vivo WBAN communications and networking: Research issues and challenges. 2015 11th International Conference on Innovations in Information Technology (IIT), Dubai, 11-16.

5. RM Shubair, H Elayan (2015) In vivo wireless body communications: State-of-the-art and future directions. Loughborough Antennas and Propagation Conference (LAPC), Loughborough, UK, 1-5.

6. H Elayan, RM Shubair, A Kiourti (2016) On graphene-based THz plasmonic nano-antennas. 16th Mediterranean Microwave Symposium (MMS), Abu Dhabi, United Arab Emirates, 1-3.

7. H Elayan, RM Shubair, JM Jornet, A Kiourti, R Mittra (2018) Graphene-based spiral nanoantenna for intrabody communication at terahertz. 2018 IEEE International Symposium on Antennas and Propagation and USNC/URSI National Radio Science Meeting, Boston, MA, USA, 799-800.

8. GE Santagati, T Melodia, L Galluccio, S Palazzo (2013) Ultrasonic networking for e-health applications. IEEE Wireless Communications 20: 74-81.

9. IF Akyildiz, F Fekri, R Sivakumar, CR Forest, BK Hammer (2012) Monaco: Fundamentals of molecular nano-communication networks. IEEE Wireless Communications 19: 12-18.

10. JM Jornet, IF Akyildiz (2011) Channel modeling and capacity analysis for electromagnetic wireless nanonetworks in the terahertz band. IEEE Transactions on Wireless Communications 10: 3211-3221.

11. S Hussein, Y Ziade, R Shubair (2019) On propagation losses due to in- vivo electromagnetic nanoscale communication. IEEE International Symposium on Antennas and Propagation and USNC-URSI Radio Science Meeting, Atlanta, GA, USA.

12. CA Balanis (2016) Antenna theory: Analysis and design. John Wiley & Sons, Singapore.

13. P Gans (1971) Vibrating molecules. Chapman and Hall London, New York.

14. K Fuwa, B Valle (1963) The physical basis of analytical

Hussein et al. Int J Nanoparticles Nanotech 2019, 5:032

ISSN: 2631-5084 | • Page 7 of 7 •

atomic absorption spectrometry. The pertinence of the beer-lambert law. Analytical Chemistry 35: 942-946.

15. K Yaws, D Mixon, W Roach (2007) Electromagnetic properties of tissue in the optical region. Proc SPIE 6435, Optical Interactions with Tissue and Cells XVIII 643507.

16. J Kindt, C Schmuttenmaer (1996) Far-infrared dielectric properties of polar liquids probed by femtosecond terahertz pulse spectroscopy. The Journal of Physical Chemistry 100: 10373-10379.

17. J Xu, KW Plaxco, SJ Allen (2006) Probing the collective vibrational dynamics of a protein in liquid water by terahertz absorption spectroscopy. Protein Sci 15: 1175-1181.

18. B Chu (1974) Laser light scattering. Elsevier.

19. TI Zohdi, FA Kuypers, WC Lee (2010) Estimation of red blood cell volume fraction from overall permittivity measurements. International Journal of Engineering Science 48: 1681-1691.

20. CB Reid, G Reese, AP Gibson, VP Wallace (2013) Terahertz time-domain spectroscopy of human blood. IEEE Journal of Biomedical and Health Informatics 17: 774-778.

21. HP Erickson (2009) Size and shape of protein molecules at the nanometer level determined by sedimentation, gel filtration, and electron microscopy. Biol Proced Online 11: 32-51.

22. H Elayan, R Shubair, J Jornet, P Johari, R Mittra (2017) Terahertz electromagnetic communication for in-vivo wireless nanosensor networks. The 2017 Progress in Electromagnetics Research Symposium (PIERS2017).